

Double-pulsed diffusional kurtosis imaging for the in vivo assessment of human brain microstructure

Edward S. Hui¹ and Jens H. Jensen^{2,3}

¹Department of Diagnostic Radiology, The University of Hong Kong, Pokfulam, Hong Kong, China, ²Department of Radiology and Radiological Science, Medical University of South Carolina, Charleston, South Carolina, United States, ³Center for Biomedical Imaging, Medical University of South Carolina, Charleston, South Carolina, United States

Purpose We have recently extended conventional single-pulsed-field-gradient (s-PFG) diffusional kurtosis imaging (DKI) to double-PFG (d-PFG) diffusion MRI sequences, with a method known as double-pulsed DKI (DP-DKI)¹. By virtue of a 6D formulation for q-space, many of the results and insights of s-PFG DKI are generalized to d-PFG. Owing to the fact that DKI isolates the second order contributions to the d-PFG signal (i.e. second order in b-value), 6D diffusional kurtosis encodes unique information beyond that available from s-PFG sequences^{1,2}. We have previously demonstrated DP-DKI of mouse brain at 7T, and it is the objective of this study to demonstrate the feasibility of in vivo human DP-DKI at 3T.

Methods Theory A detailed description of DP-DKI is given by Ref. 1. Briefly, a typical d-PFG sequence consists of 2 s-PFG blocks, one between the 90° and 180° pulses, and the other after the 180° pulse. The pulse duration δ and the diffusion time Δ are assumed to be identical for both blocks, and the interval between the end of the first and the beginning of the second s-PFG is characterized by a mixing time τ . The b-values for the 2 s-PFG blocks are $b \equiv (\gamma\delta g)^2(\Delta - \delta/3)$ and $b' \equiv (\gamma\delta g')^2(\Delta - \delta/3)$, respectively, and the corresponding 3D diffusion wave vectors are $\mathbf{q} \equiv \gamma\delta g\mathbf{n}/2\pi$ and $\mathbf{q}' \equiv \gamma\delta g'\mathbf{n}'/2\pi$. The pair of diffusion wave vectors $(\mathbf{q}, \mathbf{q}')$ can be regarded as a 6D diffusion wave vector $\tilde{\mathbf{q}} \equiv (\mathbf{q}, \mathbf{q}')$, whereby the first 3 components of $\tilde{\mathbf{q}}$ corresponds to \mathbf{q} and the last 3 components of $\tilde{\mathbf{q}}$ corresponds to \mathbf{q}' . The 6D unit vector associated with $\tilde{\mathbf{q}}$ is $\tilde{\mathbf{n}} \equiv \tilde{\mathbf{q}}/\tilde{q}$, where $\tilde{q} \equiv |\tilde{\mathbf{q}}|$. The 6D b-value of a d-PFG sequence is then: $\tilde{b} \equiv (2\pi\tilde{q})^2(\Delta - \delta/3) = b + b'$. The logarithm of d-PFG signal $\tilde{S}(\tilde{b}, \tilde{\mathbf{n}})$ can then be expanded in powers of \tilde{b} : $\ln \tilde{S}(\tilde{b}, \tilde{\mathbf{n}})/\tilde{S}(0, \tilde{\mathbf{n}}) = -\tilde{b}\tilde{D}(\tilde{\mathbf{n}}) + \tilde{b}^2\tilde{D}(\tilde{\mathbf{n}})^2\tilde{K}(\tilde{\mathbf{n}})/6 + O(\tilde{b}^3)$, where $\tilde{D}(\tilde{\mathbf{n}})$ and $\tilde{K}(\tilde{\mathbf{n}})$ are the 6D directional diffusivity and diffusional kurtosis, respectively. The directional dependence of $\tilde{D}(\tilde{\mathbf{n}})$ and $\tilde{K}(\tilde{\mathbf{n}})$ may be fully described by 6D diffusion and kurtosis tensors, which have 12 and 66 independent components, respectively. The means of the 6D tensors are estimated in lieu of the full tensors to minimize image acquisition time. These metrics can be found by first calculating $\tilde{\psi}(\tilde{b}) = \sum_{m=1}^{15} \ln \tilde{S}(\tilde{b}, \tilde{\mathbf{n}}_m)/12 + \sum_{m=16}^{21} \ln \tilde{S}(\tilde{b}, \tilde{\mathbf{n}}_m)/24 - \sum_{m=1}^3 \ln \tilde{S}(\tilde{b}, \tilde{\mathbf{n}}_m)/12$, where $\tilde{\mathbf{n}}_m$ is the set of 21 6D diffusion-encoding directions in Table 1 of Ref. (1). The means of the 6D diffusion tensor (\tilde{D}) and kurtosis tensor (\tilde{W}) can then be estimated from a quadratic fit to $\tilde{\psi}(\tilde{b}) = \ln \tilde{S}_0 - \tilde{b}\tilde{D} + \tilde{b}^2\tilde{D}^2\tilde{W}/6 + O(\tilde{b}^3)$. An analogous method has also been proposed for estimating the means of the standard 3D diffusion tensor (\bar{D}) and kurtosis tensor (\bar{W})³. MRI n = 4 healthy volunteers were scanned using 3T MRI scanner (Achieva, Philips) with an in-house d-PFG SE-EPI sequence. DWIs were acquired with 5 6D b-values (0, 500, 1000, 1500, 2000 s/mm²) along 21 diffusion-encoding directions (Table 1 of Ref. (1)) with $\delta/\Delta/\tau = 14.9/21.4/34.1$ ms, TR/TE = 5500/112 ms, FOV = 230 x 230 mm², acquisition matrix = 76 x 76, SENSE factor = 2, TH = 5 mm, BW = 3657 Hz/pixel, NEX = 2, acquisition time = 19 minutes. Post-processing Linear least square estimation of \tilde{D} and \tilde{W} , as well as of \bar{D} and \bar{W} , was performed. The conventional fractional anisotropy (FA) was also estimated from the same dataset. ROIs of the splenium of the corpus callosum (CC), putamen (PU) and thalamus (THA) were manually selected. All measurements were obtained by taking the average of all voxels in the corresponding ROIs. All computations were performed using MATLAB.

Results and Discussion Representative parametric maps are illustrated in Fig. 1. White matter (WM) and deep gray matter (GM) regions have higher $\bar{W} - \tilde{W}$ than cortical regions and ventricles. $\bar{W} - \tilde{W}$ is largely complementary to FA throughout most brain regions. Notably, $\bar{W} - \tilde{W}$ carries different information in complex WM regions, such as fanning or crossing fibers. In particular, observed $\bar{W} - \tilde{W}$ values are consistent with these brain regions having a high degree of microscopic anisotropy amid the relatively low macroscopic anisotropy as revealed by FA, and that cortical GM regions have substantially lower microscopic anisotropy. The ROI measurements for all subjects are shown in Fig. 2. The absolute difference between \bar{D} and \tilde{D} is very small (maximum difference of $0.03 \pm 0.02 \mu\text{m}^2/\text{ms}$), which is expected¹. The mean and standard deviation of the $\bar{W} - \tilde{W}$ of all subjects for CC, THA and PU are 0.22 ± 0.03 , 0.15 ± 0.03 and 0.12 ± 0.01 , respectively. Apart from mapping microscopic anisotropy, another potential application of the additional information provided by DP-DKI pertains to biophysical modeling of brain microstructure, which will be performed in future study. It is worth noting that there are other methods that allow the estimation of the microscopic anisotropy of brain tissue, including those proposed by Lawrenz and Finsterbusch⁴, Jespersen et al⁵, and Szczepankiewicz⁶. These are closely related to the framework of DP-DKI, and that the contrast of the microscopic anisotropy metric estimated by these methods are qualitatively similar to that of $\bar{W} - \tilde{W}$.

Conclusion A clinically feasible DP-DKI method has been successfully demonstrated for the in vivo assessment of the microscopic anisotropy of human brain. Microscopic anisotropy, as estimated by the rotationally invariant DP-DKI metric $\bar{W} - \tilde{W}$, reveals microstructural information that is not obtainable with conventional s-PFG diffusion MRI.

References 1) Jensen JH et al. *NMR Biomed* 2014;27(4):363-370. 2) Jespersen SN. *NMR Biomed* 2012;25(6):813-818. 3) Hansen et al. *Magn Reson Med* 2013;69(6):1754-1760. 4) Lawrenz M et al. *J Magn Reson* 2010;202(1):43-56. 5) Jespersen SN et al. *NMR Biomed* 2013;26(12):1647-1662. 6) Szczepankiewicz et al. *Neuroimage* 2014; on line.

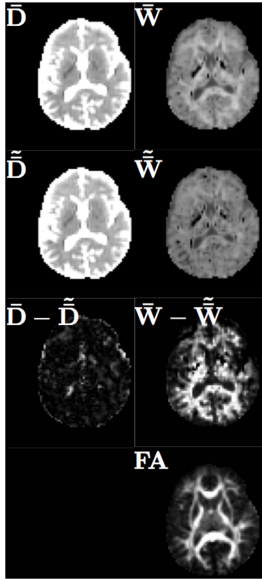


Fig. 1. \tilde{D} , \bar{D} , $\tilde{D} - \bar{D}$, \tilde{W} , \bar{W} , $\tilde{W} - \bar{W}$ and FA maps. Scale for MD maps: 0 – 1.4 $\mu\text{m}^2/\text{ms}$; MD difference: 0 – 0.3 $\mu\text{m}^2/\text{ms}$; kurtosis: 0 – 1.4; kurtosis difference: 0 – 0.3; and FA: 0 – 0.6.

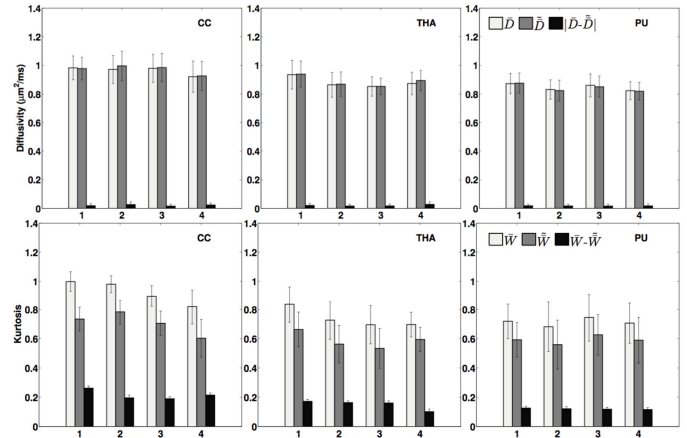


Fig. 2. \bar{D} , \tilde{D} , $|\bar{D} - \tilde{D}|$ (upper row), \bar{W} , \tilde{W} and $\bar{W} - \tilde{W}$ (lower row) measurements which are expressed as mean and standard deviation of all values in the corresponding ROI for each subject.